TISSUE ENGINEERING: Part A
Volume 20, Numbers 3 and 4, 2014

DOI: 10.1089/ten.tea.2013.0122

Epithelial-Differentiated Adipose-Derived Stem Cells Seeded Bladder Acellular Matrix Grafts for Urethral Reconstruction: An Animal Model

Hongbin Li, PhD,[1,2] Yuemin Xu, PhD, MD,[1,2] Hong Xie, PhD,[1,2] Chao Li, PhD,[1,2] Lujie Song, PhD,[1,2] Chao Feng, PhD,[1,2] Qin Zhang, PhD,[1,2] Minkai Xie, PhD,[1,2] Ying Wang, PhD,[1,2] and Xiangguo Lv, PhD[1,2]

The limited amount of available epithelial tissue is considered a main cause of the high rate of urethral reconstruction failures. The aim of this study was to investigate whether epithelial-differentiated rabbit adipose-derived stem cells (Epith-rASCs) could play a role of epithelium *in vivo* functionally and be a potential substitute of urothelium. Substitution urethroplasty was performed to repair an anterior urethral defect in male New Zealand rabbits using Epith-rASCs seeded bladder acellular matrix grafts (BAMGs) after 5-bromo-2′-deoxyuridine (BrdU) labeling, based on the *in vitro* epithelial induction system we previously described. Urethroplasty with cell-free BAMGs and with undifferentiated rASCs (Und-rASCs) seeded BAMGs were performed as controls. After surgery, a notable amelioration of graft contracture and recovery of urethral continuity were observed in the Epith-rASCs/BAMG group by retrograde urethrograms and macroscopic inspection. Immunofluorescence revealed that the BrdU-labeled Epith-rASCs/Und-rASCs colocalized with *cytokeratin 13* or *myosin*. Consistent with the results of western blotting, at early postimplantation stage, the continuous epithelial layer with local multilayered structure was observed in the Epith-rASCs/BAMG group, whereas no significant growth and local monolayer growth profile of epithelial cells were observed in the BAMG and Und-rASCs/BAMG group, respectively. The results showed that Epith-rASCs could serve as a potential substitute of urothelium for urethral tissue engineering and be available to prevent lumen contracture and subsequent complications including recurrent stricture.

Introduction

Urethral stricture caused by trauma, cancer, or inflammation is considered a challenging disease for reconstructive urologists. At present, urethroplasty is generally considered the optimal choice for urethral repair in most cases. But clinically, the limited amount of substitution tissue is a main cause of the high rates of repair failures.[1,2]

For solving the problem, studies have been performed to find an ideal substitution material for urethroplasty using tissue engineering technology.[3–6] Composite materials seeded by autologous epithelium have been tried in preclinical studies.[7–9] But *in vitro* cellular senescence, however, prevents their clinical use.

Mesenchymal stem cells have been regarded as a potential alternative for tissue repair and regeneration research based on the characteristics of self-renewal and multipotent differentiation capacity.[10–13] Among which, adipose-derived stem cells (ASCs) have the advantage of being harvested in abundant quantity and causing less trauma to donor site, and recent studies show that ASCs can differentiate toward epithelial lineage under the synergistic stimulation of contributing factors.[14,15] Furthermore, human adipose-derived stem cells (hASCs) in direct coculture with uroepithelial cells were observed to express urothelial-specific genes uroplakin Ib and uroplakin II.[16]

In our earlier study, an *in vitro* three-dimensional (3D) culture system was established to induce epithelial differentiation of rabbit adipose-derived stem cells (rASCs). After induction, rASCs were observed to display a stratified epithelial-like morphology, with expression of early epithelial-specific proteins.[17] As a continuing research, the research question of the current study is whether the Epith-rASCs could serve *in vivo* as a potential substitute of urothelium for urethral reconstruction.

[1]Department of Urology, Sixth People's Hospital, Jiao Tong University of Shanghai, Shanghai, P.R. China.
[2]Shanghai East Institute for Urologic Repair and Reconstruction, Shanghai, P.R. China.

Herein, substitution urethroplasty in male New Zealand rabbits was performed using epithelial-differentiated rASCs (Epith-rASCs) seeded bladder acellular matrix grafts (BAMGs) after 5-bromo-2′-deoxyuridine (BrdU) labeling of the implanted cells. Histological and functional evaluation revealed that the Epith-rASCs could produce functional effects of epithelium in a suitable *in vivo* microenvironment and also be helpful to prevent the excessive contracture and fibrosis on the lumen of urethral substitute.

Materials and Methods

Isolation and culture of rASCs in vitro

All the experimental protocols were approved by the Animal Care and Use Committee in our institution. The adipose tissues were obtained from the dorsocervical subcutaneous region of male New Zealand rabbits. The isolation and culture of rASCs were performed, as previously described.[18,19] After rinsing in 0.25% chloromycetin and phosphate-buffered saline (PBS), the fresh adipose tissues were cut into small pieces and then treated with 0.10% collagenase I (Worthington Biochemical Corp.) under shaking at 37°C for 60 min. After digestion, the collagenase I was neutralized with low-glucose Dulbecco's modified Eagle's medium (LG-DMEM; Gibco) supplemented with 10% fetal bovine serum (FBS; Gibco), and the suspension was filtered through a 200-μm nylon mesh to remove the undigested tissue and then centrifuged at 1200 *g* for 10 min. The pellet was resuspended in LG-DMEM supplemented with 10% FBS. The cells were cultivated at a density of 4×10^4 cells/cm^2, and the media was changed every 3 days. The cells were passaged at 70–80% confluence. The rASCs of passage 3 were used for the study. The characterization of isolated cells was determined by their CD marker profile in our previous study.[17]

Epithelial differentiation of rASCs in a 3D culture system and characterization of the Epith-rASCs

A 3D culture system was established to imitate the *in vivo* epithelial-specific microenvironment for epithelial differentiation of rASCs. Details of the system were previously described.[17] Briefly, in the system, rASCs were seeded on the upper side of the membrane of a Millicell insert (1.0-μm pore size; Millpore Co.) coated with 0.10% collagen type IV (Sigma-Aldrich). To create an air–liquid interface (ALI) culture condition, the inducing medium (described below) in basolateral compartment was raised to reach the level of the membrane, and then, the cells were exposed to the air with 5% CO_2 with 95% relative humidity while fed from the medium underneath.

Based on the *in vitro* results, we chose the optimal induction method for further study. Under the ALI culture condition, resuspended rASCs (passage 3) were cultured at a seeding density of 3×10^4 cells/cm^2 in LG-DMEM supplemented with 2% FBS, 2.5 μM all-trans retinoic acid (Sigma-Aldrich), 20 ng/mL epidermal growth factor (Peprotech), 10 ng/mL hepatocyte growth factor (Peprotech), 10 ng/mL keratinocyte growth factor (Peprotech), and 0.5 μg/mL hydrocortisone (Sigma-Aldrich). After 12 days from the initial inducing, the Epith-rASCs were prepared for the *in vivo* study.

After induction, proteinic and genetic analysis of the epithelial phenotypes and alpha-smooth muscle actin (α-SMA), and detections of the growth pattern and viability of cells have been performed for a full-scale assessment. rASCs displayed a stratified epithelial-like morphology, with expression of cytokeratin 19 (an early epithelial marker) and weak cytokeratin 13 (an epithelial marker mainly expressed in mucosal epithelium). The expression of α-SMA decreased, but almost no expression of involucrin (a terminal epithelial marker) was detected. Moreover, no significant decrease in cell proliferation and viability was observed after induction.[17]

BrdU labeling of the Epith-rASCs

The Epith-rASCs were labeled with BrdU (Sigma-Aldrich), for investigating the differentiation and proliferation profiles of implanted cells. After induction, the cells were collected and resuspended in the keratocyte serum-free medium (KSFM; Gibco) under the ALI culture condition and then incubated with 15 μM BrdU when 70% confluence was reached. The undifferentiated rASCs (Und-rASCs) were labeled with BrdU as a control group.

After 48 h incubation, cells were assessed for BrdU incorporation and cell viability by immunofluorescent staining and Hoechst 33258 assay, respectively.

BAMG preparation and evaluation

The bladders of male New Zealand rabbits were aseptically obtained and then BAMGs were prepared as previously described.[9,20] After washing with double distilled water for 24 h, the isolated matrices were treated using 1% Triton X-100 (Sigma) and 0.1% ammonium hydroxide with continuous shaking for 14 days to induce cell lysis. The solution was refreshed every 3 days. The resultant BAMGs were washed with PBS for three times and stored in 0.25% chloramphenicol solution at 4°C before use.

The characterization of BAMGs, including hematoxylin and eosin staining, Masson staining, and scanning electron microscopy, was performed as previously described (data not shown)[9,21,22] to study the texture and ultrastructure of the matrices and to identify whether the cellular components were removed.

Rabbit urethroplasty with rASCs seeded BAMGs

BAMGs were irradiated by ultraviolet light for 12 h after three washes before use. After labeling with BrdU, the Epith-rASCs were seeded onto 2.0×0.8 cm^2 BAMGs at 5×10^6 cells/cm^2. The compound grafts were cultured at air–liquid level in the KSFM for 7 days, with the culture medium refreshed every 2 days. The Und-rASCs were seeded onto BAMGs as a control. After culture, the grafts were assessed by transmission electron microscopy.

Thirty-six rabbits were divided into three groups of 12 each. The BAMG group (control group 1) underwent substitution urethroplasty using cell-free BAMGs; the Und-rASCs/BAMG group (control group 2) with Und-rASCs seeded BAMGs; the Epith-rASCs/BAMG group (study group) with Epith-rASCs seeded BAMGs (Fig. 1). The rabbits were anesthetized with pentobarbital, and an 8F urethral catheter was placed. The urethra was mobilized through the ventral midline incision of the penile shaft.

FIG. 1. The rabbits in the Epith-rASCs/BAMG group underwent substitution urethroplasty using Epith-rASCs seeded BAMGs. After a urethral defect with a mean length of 2.0 cm and width of 0.8 cm was created in the rabbits' ventral anterior urethra, the compound graft was placed over the defect using 6-0 vicryl sutures. Epith-rASCs, epithelial-differentiated rabbit adipose-derived stem cells; BAMG, bladder acellular matrix graft. Color images available online at www.liebertpub.com/tea

A urethral defect with a mean length of 2.0 cm and width of 0.8 cm was created in the rabbits' ventral anterior urethra, about 2.5 cm from the external urethral meatus. The compound graft was placed over the defect using 6-0 vicryl sutures. The catheter remained for 14 days to provide bladder drainage after the surgery.

Three animals in each group were euthanized at 2 weeks, 1 month, 2 months, and 6 months postimplantation. The entire urethra was extirpated for the examinations.

Cell proliferation assay

Cell proliferation of Epith-rASCs/Und-rASCs was assayed before and after BrdU labeling. The cells at different time points were crushed for full lysis with proteinase K (Sigma-Aldrich) at 56°C overnight. The resultant mixture was subjected to centrifugation, and then, aliquots of the supernatants were mixed with Hoechst 33258 dye solution (Sigma-Aldrich). DNA content was quantified spectrofluorometrically using a Varioskan multimode detection reader (Thermo Electron). The DNA standard curve was generated by lysing serial dilutions of a known concentration of rASCs.

Analysis of transmission electron microscopy

Transmission electron microscopy (CM 120; Philips) examination was performed for the evaluation of the grafts after cell seeding. The samples were fixed with 2% glutaraldehyde, postfixed with 1% osmium tetraoxide, stained with 0.5% uranyl acetate, and dehydrated with acetone. After being embedded in resin, the grafts were cut in cross section to observe the cellular growth profile after 7 days of *in vitro* culture.

Retrograde urethrography and macroscopic inspection

Retrograde urethrograms were performed for the assessment of urethral caliber before animals were euthanized. The appearance of retrieved urethra was evaluated by macroscopic inspection.

Multicolor immunofluorescent evaluation

Immunofluorescent staining of retrieved urethra was performed to evaluate the development of implanted grafts at each time point postimplantation. Animals were euthanized, and the fresh implanted grafts were harvested. After frozen in OCT compound by liquid nitrogen, 6- to 8-μm-thick cryosections were cut. Sections were dried for 30 min and then washed with PBS for three times. After permeabilization with 0.5% Triton X-100 for 20 min at room temperature, the specimens were incubated with 2 M HCl for 30 min at 37°C for BrdU detection and incubated with the horse serum blocking solution (2% horse serum, 1% bovine serum albumin) for 30 min to reduce the nonspecific binding. Subsequently, the sections were incubated with first primary antibody (anti-cytokeratin 13, anti-myosin) for 60 min at 37°C, washed three times, and incubated with first secondary antibody (Alexa Fluor 488 goat anti-mouse IgG) for 30 min at 37°C, then incubated with second primary antibody (anti-BrdU) for 60 min and second secondary antibody (Alexa Fluor 568 goat anti-rat IgG) for 30 min at 37°C after three washes each. Cell nucleus was stained with Hoechst 33258.

The specimens were examined using the fluorescence microscopy (Nikon 80i; Nikon) and confocal microscopy (LSM 710; Zeiss). A blank control was used to eliminate potential cross-reactivity with the rabbit proteins.

Primary antibodies: anti-BrdU (rat monoclonal IgG, ab6326; Abcam), anti-cytokeratin 13 (mouse monoclonal IgG, sc-57003; Santa Cruz), anti-myosin (mouse monoclonal IgG, ab680; Abcam); secondary antibodies: Alexa Fluor 488 goat anti-mouse IgG (Invitrogen), Alexa Fluor 568 goat anti-rat IgG (Invitrogen).

Western blot analysis

Western blot analysis was performed to measure the relative expression level of *cytokeratin 19* and *cytokeratin 13* of retrieved urethra. The urethra sample of $0.5 \times 0.5 \times 0.1\ cm^3$ each was added into 300 μL lysis buffer (50 mM Tris-HCl, pH 8.0, 150 mM NaCl, 1% NP-40, 0.5% sodium deoxycholate, 0.1% sodium dodecyl sulfate, 1.0 mM phenylmethanesulfonyl fluoride) for extracting proteins after being cut into small pieces, and then, proteins were size fractionated using sodium dodecyl sulfate–polyacrylamide gel electrophoresis and transferred to nitrocellulose membranes (Bio-Rad) (each protein sample from three animals was extracted at each time point in various groups, respectively). After blocking with TBST (Tris-buffered saline with 0.1% Tween-20) containing 5% nonfat dry milk and 2% bovine serum albumin for 1 h at room temperature, the membranes were incubated with primary antibodies at 4°C overnight and subsequently with IRDye 800-conjugated secondary antibody (goat anti-mouse; Rockland) for 1 h at room temperature. Proteins were visualized by the Odyssey Infrared Imaging System (LI-COR Biosciences). Anti-GAPDH antibody was used as a protein loading control.

Primary antibodies: anti-cytokeratin 19 (mouse monoclonal IgG, ab77983; Abcam), anti-cytokeratin 13 (mouse monoclonal IgG, sc-57003; Santa Cruz).

Image analysis and statistical analysis

After immunofluorescent staining of retrieved urethra was performed, five fields (20× objective view) per slide at each time point in various groups were taken under microscopy. The positive areas of *cytokeratin 13* staining were measured by KS400 Image Analysis System (Carl Zeiss, German). The relative positive area per field was used for coverage assessment of epithelial cells on the surface of lumen.

Data were presented as mean ± standard deviation from three or more experiments. Independent-samples *T*-tests assuming equal variance were performed using SPSS 11.0 software (SPSS, Inc.) for statistical analysis. A *p*-value of less than 0.05 was considered statistically significant.

Results

Identification of BrdU-labeled cell in vitro

BrdU incorporation of the cells was assessed after 48 h incubation. Immunofluorescence revealed that both Epith-rASCs and Und-rASCs (labeled with *cytokeratin 19*) colocalized with BrdU expression (Fig. 2A). Ten different fields (10× objective view) in each group were taken under microscopy for the counting of $BrdU^+$ rASCs. Data were presented as mean ± standard deviation. The percentage of $BrdU^+$ cells was 94.17% ± 2.26% in the Epith-rASCs group and 94.68% ± 1.74% in the Und-rASCs group. After being passaged two times, BrdU incorporation assessment was repeated and a similar outcome was observed (data not shown).

Hoechst 33258 assay was performed for the evaluation of cell proliferation and viability. As shown in Figure 2B, after 48 h incubation with BrdU, no significant decrease in cell proliferation rate was observed. The cell numbers of labeled Epith-rASCs/Und-rASCs were observed to keep on increasing after seeding, reached a peak at day 7 or 6, respectively, which were similar to the cells growth in unlabeled state.

Assessment of the compound grafts

Under transmission electron microscopy, a stratified cellular growth pattern was observed in both compound grafts (Fig. 3A). Epith-rASCs in some areas were found to infiltrate into the underlayer of the BAMGs after 7 days of *in vitro* culture (Fig. 3B), which was also observed in Und-rASCs seeded BAMGs (data not shown).

Evaluation of the implanted grafts after urethroplasty in vivo

Retrograde urethrograms were performed for the assessment of urethral caliber and identification of postoperative

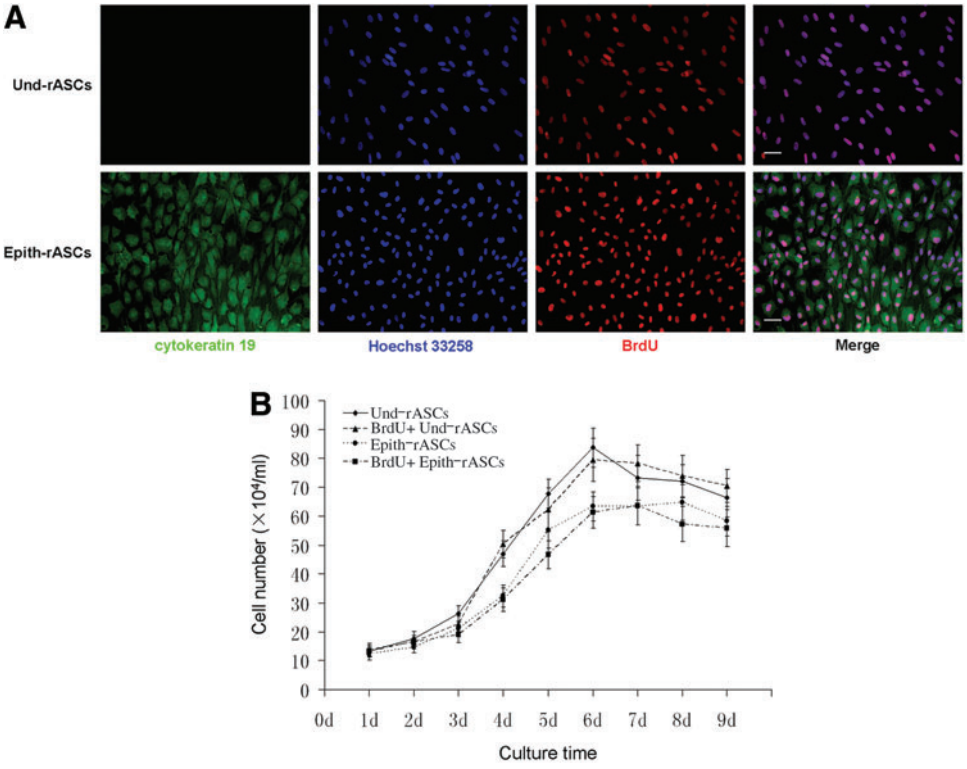

FIG. 2. BrdU incorporation and cell viability assessment of Und-rASCs and Epith-rASCs after 48 h incubation with BrdU. **(A)** Immunofluorescent staining of the Und-rASCs and Epith-rASCs after labeling with BrdU. The Und-rASCs and Epith-rASCs (labeled with cytokeratin 19) colocalized with BrdU expression. Cytokeratin 19: green; nuclei of all the cells stained with Hoechst 33258: blue; nuclei of BrdU-labeled cells: red. Scale bars: 50 μm. **(B)** Proliferation of rASCs before and after labeling with BrdU, determined by DNA assay using Hoechst 33258. BrdU, 5-bromo-2′-deoxyuridine; Und-rASCs, Und-rASCs before labeling with BrdU; $BrdU^+$ Und-rASCs, Und-rASCs after labeling with BrdU; Epith-rASCs, Epith-rASCs before labeling with BrdU; $BrdU^+$ Epith-rASCs, Epith-rASCs after labeling with BrdU; Und-rASCs, undifferentiated rASCs. Color images available online at www.liebertpub.com/tea

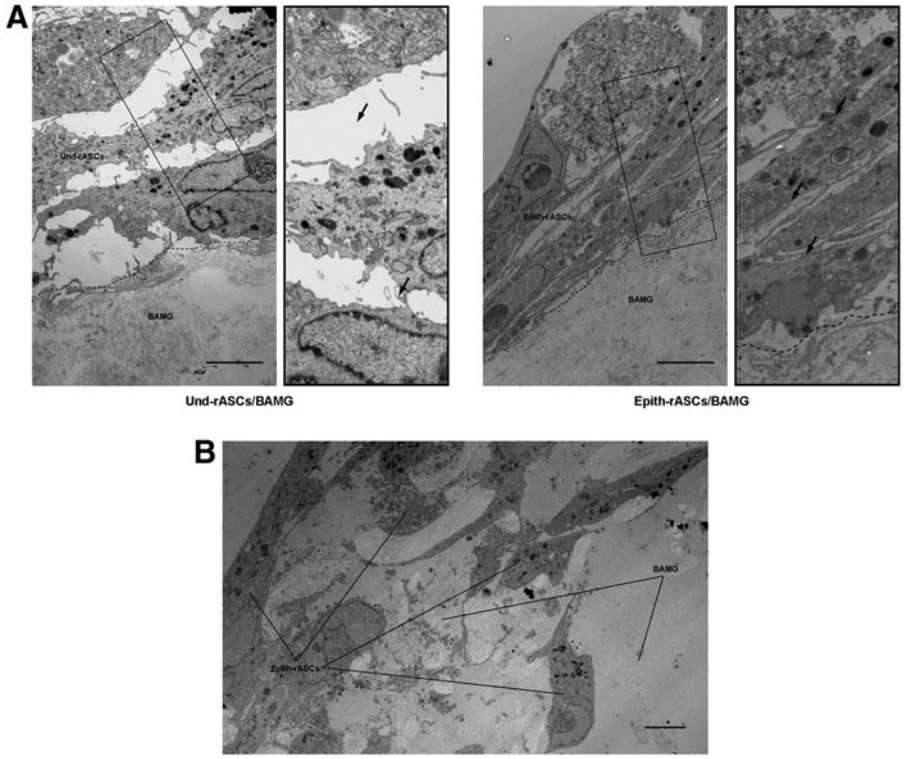

FIG. 3. The compound grafts were evaluated by transmission electron microscopy after 7 days of *in vitro* culture. **(A)** A stratified cellular structure was observed in both Und-rASCs seeded and Epith-rASCs seeded BAMGs. The Und-rASCs grew in a loosely organized fashion in the intercellular space, whereas the Epith-rASCs grew in a relatively compact fashion. The enlarged images of black rectangle box shown in the right side of the original figure. Arrow indicates the intercellular space. **(B)** The Epith-rASCs in some areas were detected to infiltrate into the underlayer of the BAMGs. Scale bars: 5 μm.

complications, including fistula and diverticula (Fig. 4). Remarkable urethral strictures were observed in both the BAMG and Und-rASCs/BAMG groups at 2 weeks and 1 month postimplantation (urethrocutaneous fistula developed in one Und-rASCs/BAMG group rabbit), which ameliorated but were still visible at 6 months postimplantation. In the Epith-rASCs/BAMG group, a mild stricture of urethra was observed at 2 weeks postimplantation, and at 1 month postimplantation, the stricture was significantly improved and the urethral caliber was close to normal. No recurrent strictures or other complications were observed at 2 and 6 months postimplantation.

Excessive contracture and fibrosis of the urethral lumen was observed in both control groups soon after the surgery (Fig. 5). Slight improvement was seen in the Und-rASCs/BAMG group at 2 and 6 months postimplantation, although the urethral continuity was still not recovered. In the Epith-rASCs/BAMG group, a mild urethral contracture was observed at 2 weeks postimplantation, which was markedly improved after several months, and amelioration in urethral continuity was shown at 6 months postimplantation.

Immunofluorescence of urethral tissue revealed no significant growth of epithelial cells (labeled with *cytokeratin 13*) in the BAMG group at early postimplantation stage, whereas in the Und-rASCs/BAMG group, BrdU-labeled Und-rASCs were observed to colocalize with *cytokeratin 13*, and the newly differentiated epithelial cells were observed to form a monolayer structure on the surface of local lumen at 1 and 2 months postimplantation (Fig. 6). In the Epith-rASCs/BAMG group, the urethral surface was covered with continuous epithelial layer at 2 weeks postimplantation, which also colocalized with BrdU-labeled Epith-rASCs. At 1 and 2 months postimplantation, compared with the occasional or discontinuous growth profile of epithelium in control groups, local multilayered epithelial cells were formed when the Epith-rASCs were chosen. A reduction in the number of BrdU-labeled cells was observed after 1 month of chase compared with that of 2 weeks, and at 6 months postimplantation, no BrdU labeling could be detected, but by single-parameter analysis of *cytokeratin 13* expression, although not like the regular stratified epithelial layers of native urethra, multilayered structure of epithelial cells was significantly formed in the Epith-rASCs/BAMG group, which was distinct from the controls. Furthermore, by confocal orthogonal slices, colocalization of BrdU with *cytokeratin 13* in the Epith-rASCs/BAMG group could be observed from x-y cross section, and the orthogonal projection of x-z and y-z cross-sectional cuts of neourethral lumen (Fig. 7A). Also, a direct-viewing structure of epithelial layers colocalized with BrdU labeling could be obtained from the 3D image of urethral tissue (Fig. 7B).

The image analysis of epithelial areas in *cytokeratin 13* staining was shown in Figure 8. From the result, relative positive areas in the two rASCs implantation groups were significantly enhanced, compared with the baseline expression in the BAMG group in the early stage (2 weeks postimplantation in the BAMG, Und-rASCs/BAMG, and Epith-rASCs/BAMG group, respectively: $121.214 \pm 21.459\ \mu m^2$, $1079.186 \pm 169.634\ \mu m^2$, $2726.494 \pm 479.153\ \mu m^2$; 1 month postimplantation: $283.143 \pm 34.638\ \mu m^2$, $1735.474 \pm 266.721\ \mu m^2$, $3780.357 \pm 316.832\ \mu m^2$). At 6 months postimplantation, the epithelial area in the Epith-rASCs/BAMG group increased to 4.45-fold compared with that in the BAMG group (BAMG group: $1763.757 \pm 233.539\ \mu m^2$, Epith-rASCs/BAMG group: $7847.140 \pm 893.774\ \mu m^2$, $p < 0.05$).

Cytokeratin 19 expression was detected in the Epith-rASCs/BAMG group at 1 month postimplantation by western blot analysis, whereas almost no expression of *cytokeratin 19* in

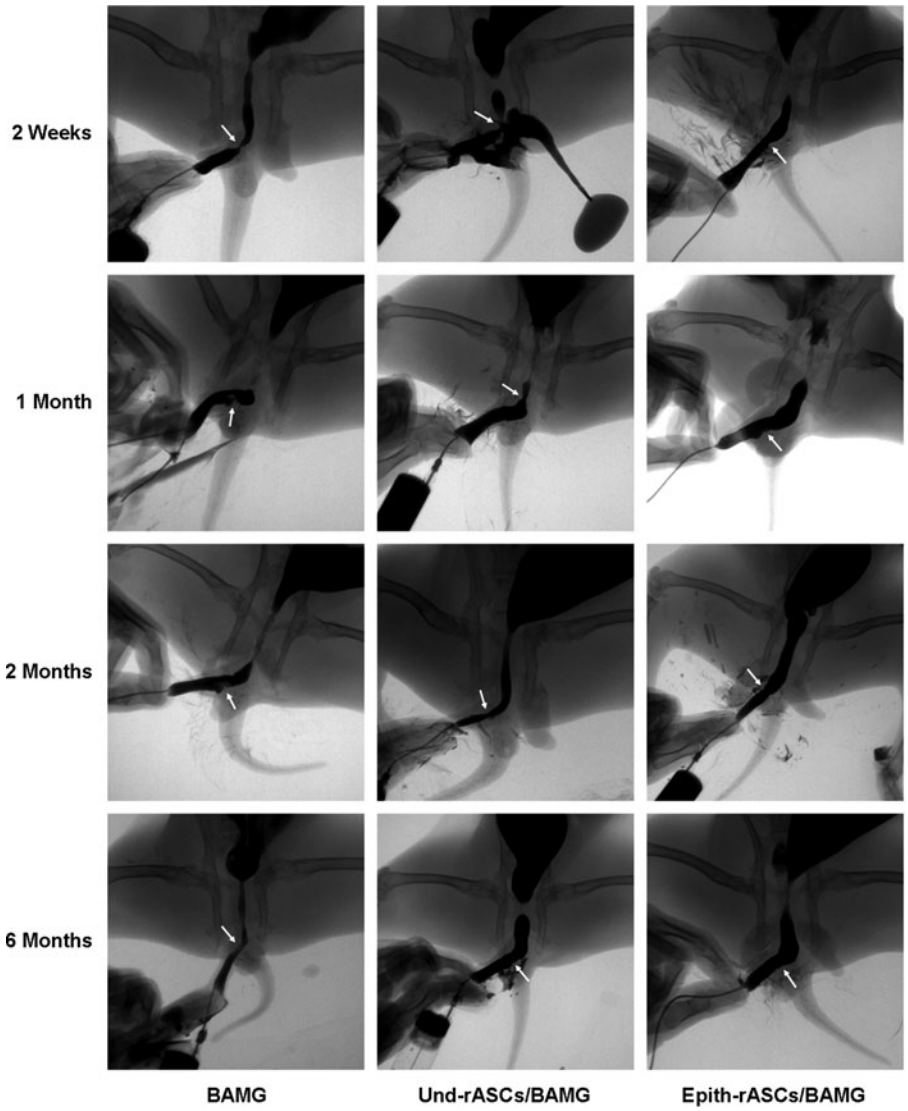

FIG. 4. Retrograde urethrograms were performed for the assessment of urethral caliber at 2 weeks, 1 month, 2 months, and 6 months postimplantation. Urethral strictures were observed in both the BAMG and Und-rASCs/BAMG groups at 2 weeks and 1 month postimplantation (urethrocutaneous fistula developed in one animal in the Und-rASCs/BAMG group); at 2 months postimplantation, the stricture of the urethra was slightly improved compared with the formers. In the Epith-rASCs/BAMG group, a mild stricture of the urethra was observed at 2 weeks postimplantation, and 1 month after the surgery, the stricture was significantly improved. Arrow indicates the replaced part of urethra.

both the BAMG and Und-rASCs/BAMG groups at the same time point (Fig. 9). At 6 months postimplantation in the two rASCs implantation groups, especially with Epith-rASCs implantation, a remarkable increase in *cytokeratin 19* expression was detected compared with the BAMG group. In contrast to *cytokeratin 19*, a similar relative expression level of *cytokeratin 13* was detected in the Epith-rASCs/BAMG group at 1 and 6 months postimplantation, whereas the expression of cytokeratin 13 in the two control groups kept in a low level.

In addition, as shown in Figure 6, BrdU-labeled implanted cells could be observed throughout the urethral surface and stroma in both rASCs implantation groups. Thus, for the purpose of investigating whether smooth muscle cell (SMC) differentiation potential of rASCs would contribute to the reformation of muscle bundles of the neourethra *in vivo* microenvironment, detection of *myosin* expression (a late marker of SMC differentiation) was performed. In the Epith-rASCs/BAMG group, BrdU labeling was observed to colocalize with local expression of *myosin* in the urethral stroma (Fig. 10A, B). At 6 months postimplantation, more extensive expression of *myosin* was observed in both rASCs implantation groups than that in the BAMG group (Fig. 10C–E). But compared with native urethra, the muscular layers in both rASCs implantation groups were formed in a random and irregular fashion (Fig. 10C, D, F).

Discussion

Based on previous studies and our experience, epithelial layers can restrain the local infiltration of inflammatory cells and fibroblasts of urethral lumen, indicating that a lack of sufficient epithelial tissue might contribute to the development of stricture after urethral reconstruction.[9,23] In today's clinical procedures, multiple autologous flaps or mucosa grafts are used for substitution urethroplasty. But the limited amount of autologous tissue and trauma at donor sites restrict the application of the surgical option.

In previous studies, acellular matrix grafts have been applied for the repair of urethral stricture and fistula.[24,25] But in the cases reported by Hauser *et al.*, recurrent stricture developed in 4 of 5 patients when it came to a longer urethral stricture (range 3.5–10 cm).[26] The preclinical[7–9] and

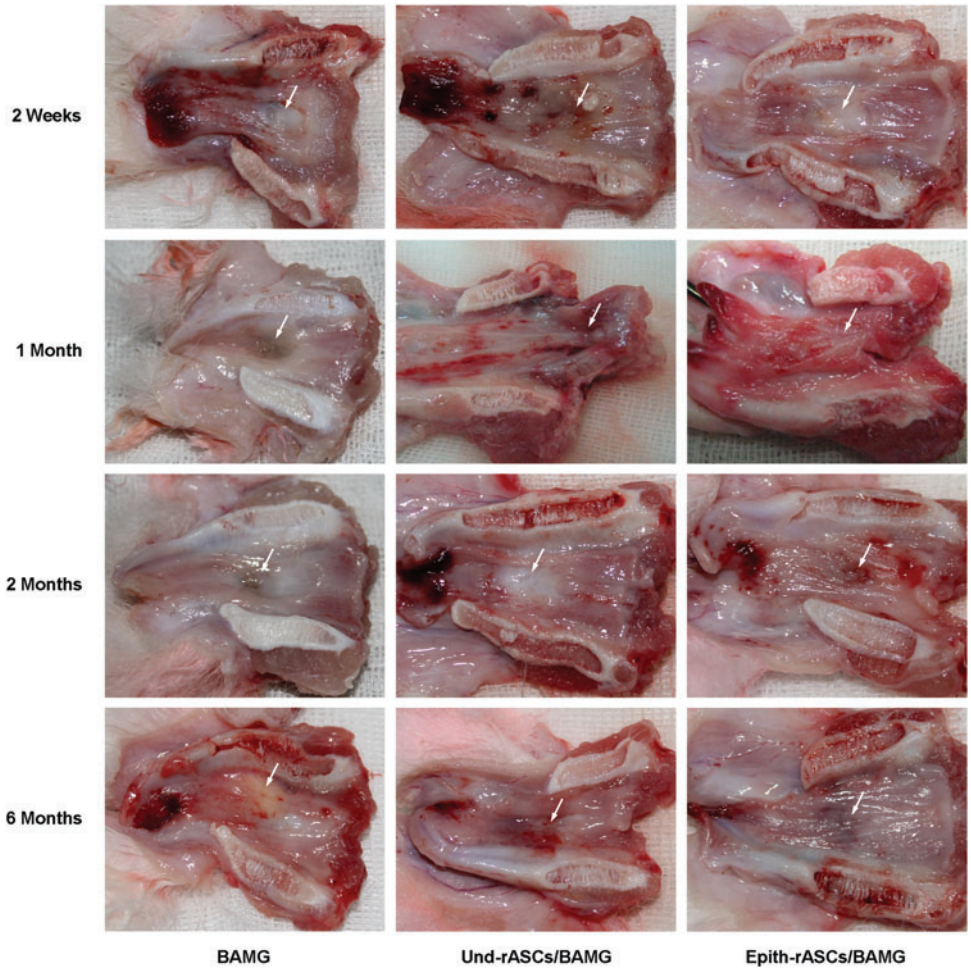

FIG. 5. Macroscopic inspection of retrieved urethra at 2 weeks, 1 month, 2 months, and 6 months postimplantation. Excessive scarring and contracture of the urethral lumen at operative site was observed in the BAMG group at 2 weeks postimplantation, followed by progressive fibrosis in the next several months. Similar contracture and fibrosis was observed in the Und-rASCs/BAMG group soon after the surgery, which improved slightly by 2 months postimplantation. In the Epith-rASCs/BAMG group, a mild contracture of the urethral lumen was observed at 2 weeks postimplantation, which was markedly improved at 2 and 6 months postimplantation. Arrow indicates the replaced part of urethra. Color images available online at www.liebertpub.com/tea

clinical[27] trials involving autologous epithelium as seed cells proved that tissue-engineered epithelial graft is a suitable substitution material for urethral reconstruction. But according to the literature[28] and our earlier work, considering the cellular senescence and subsequent difficulty in amplification of epithelium *in vitro*, it might be hard to obtain sufficient cells to meet clinical demands and the decrease in cell proliferation and viability after being passaged would have an adverse impact on the repair in the cases with complex and long-segment urethral strictures. Also in reconstruction with oral keratinocyte, buccal complications including oral ulcer and scar contracture might be caused, and a history of oral disease would also restrict the application of the cells.

ASCs have shown a high proliferative potential and multidifferentiation potential into epithelial lineage[14,15,29] besides myogenic,[30,31] osteogenic,[18,32], and chondrogenic lineages.[33,34] And the harvesting of ASCs would cause less trauma to donor site compared with autologous epithelium. In our pilot study, rASCs were demonstrated to differentiate into epithelial lineage, with characteristic stratified polygonal morphology and expression of *cytokeratin 19* and weak *cytokeratin 13*.[17] The aim of this study was to investigate whether the Epith-rASCs could be a potential source of seed cells for urethral reconstruction.

From the result of transmission electron microscopy and our experience,[9] BAMG was proved to be available for urethral tissue engineering after cells seeding. In the experiment, Epith-rASCs seeded BAMGs were applied for the repair of anterior urethra defect in rabbit models. As shown in urethrograms and macroscopic inspection, a notable amelioration of graft contracture was observed in the Epith-rASCs/BAMG group, in contrast to the two controls. Also with Epith-rASCs seeded grafts, the urethral continuity was almost recovered at 6 months postimplantation, which showed the feasibility of application of epithelial-differentiated ASCs as a substitute of urothelium.

Histologically, implanted cells expressing *cytokeratin 13* incorporated BrdU after the surgery in the two rASCs implantation groups (Fig. 6), suggesting that rASCs could differentiate toward epithelium in an epithelial-specific microenvironment *in vivo*. Furthermore, consistent with the relative expression level of cytokeratins detected by western blot analysis, the data showed compared with the discontinuous growth profile of epithelium in the Und-rASCs/BAMG group, the continuous epithelial layer with local multilayered structure was observed at 1 month postimplantation in the Epith-rASCs/BAMG group. Thus, considering the ideal result of urethrograms and macroscopy in study group, we speculated that epithelial structure originating from the Epith-rASCs plays a critical role in preventing fibrosis of the lumen. Also, from the image analysis of epithelial areas, staying in a lower rate of epithelium proliferation in the early stage (within 1 month

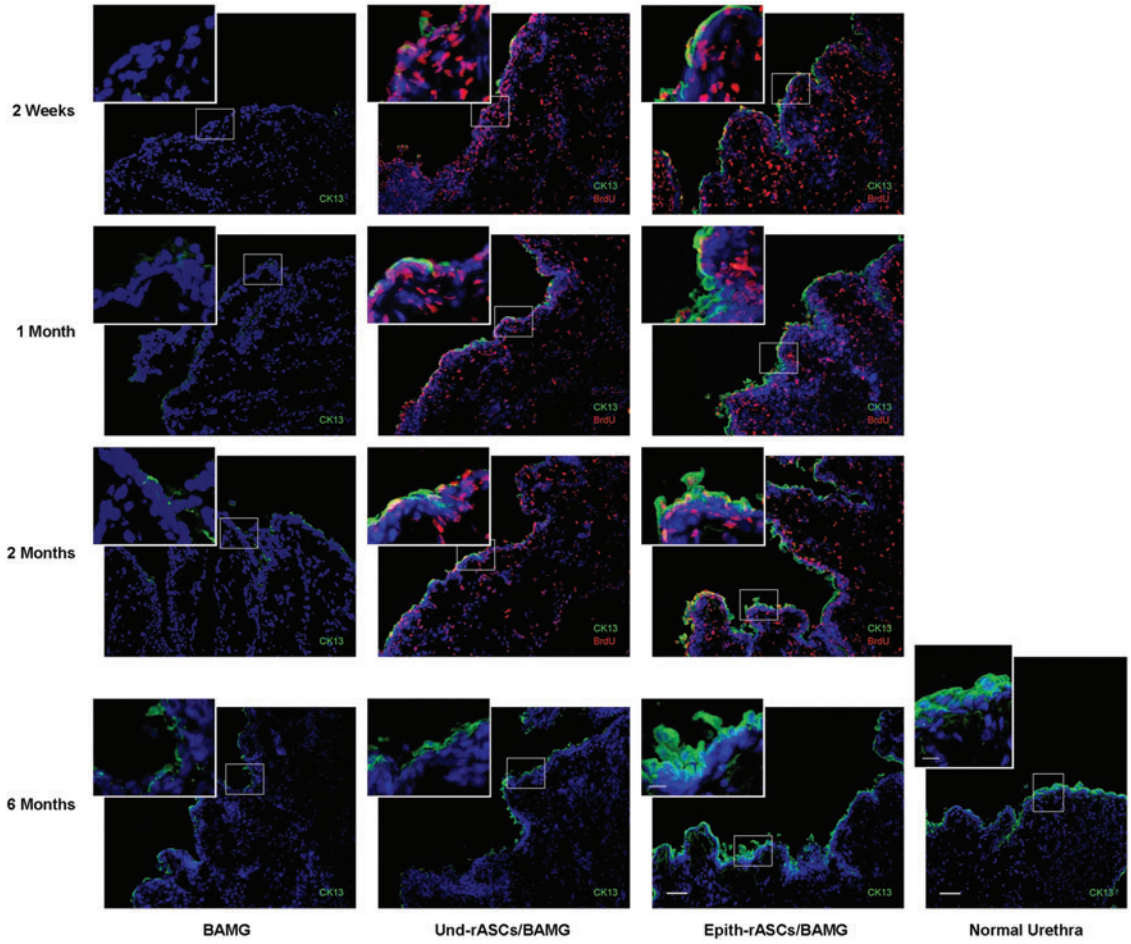

FIG. 6. Immunofluorescent evaluation of retrieved urethra at 2 weeks, 1 month, 2 months, and 6 months postimplantation. Normal urethra served for the comparison. In the BAMG group, almost no epithelial cells (labeled with *cytokeratin 13*) were observed on the urethral surface at 2 weeks postimplantation. Local discontinuous growth of epithelial cells was observed at 1 and 2 months postimplantation. In the Und-rASCs/BAMG group, occasional epithelial cell growth was observed at 2 weeks postimplantation. At 1 and 2 months postimplantation, a monolayer of epithelial cells was observed on the surface of local lumen, which colocalized with BrdU-labeled Und-rASCs. In the Epith-rASCs/BAMG group, the urethral surface was covered with continuous epithelial layer at 2 weeks postimplantation, which also colocalized with BrdU-labeled Epith-rASCs. At 1 and 2 months postimplantation, a local multilayered epithelial cells could be observed, and the multilayered structure of cells was more significant at 6 months postimplantation compared with the control groups (at 6 months postimplantation, no BrdU labeling could be detected by immunofluorescent staining). CK13: *cytokeratin 13*, green; nuclei of BrdU-labeled cells: red; nuclei of all the cells stained with Hoechst 33258: blue. Scale bars: 50 μm for original figures; 12.5 μm for insets. Color images available online at www.liebertpub.com/tea

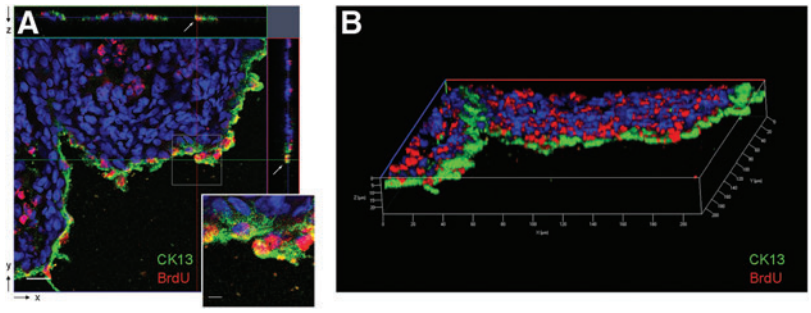

FIG. 7. Confocal microscopy of *cytokeratin 13* expression in implanted cells in the Epith-rASCs/BAMG group. **(A)** The image of confocal orthogonal slices showed the colocalization of BrdU with *cytokeratin 13* from x-y cross section, and the orthogonal projection of both x-z and y-z cross-sectional cuts (white arrow) at 1 month postimplantation. **(B)** The colocalization of BrdU with *cytokeratin 13* was also shown from the 3D view of urethral tissue. CK13: *cytokeratin 13*, green; nuclei of BrdU labeled cells: red; nuclei of all the cells stained with Hoechst 33258: blue. Scale bars: 20 μm for original figure; 5 μm for inset. Color images available online at www.liebertpub.com/tea

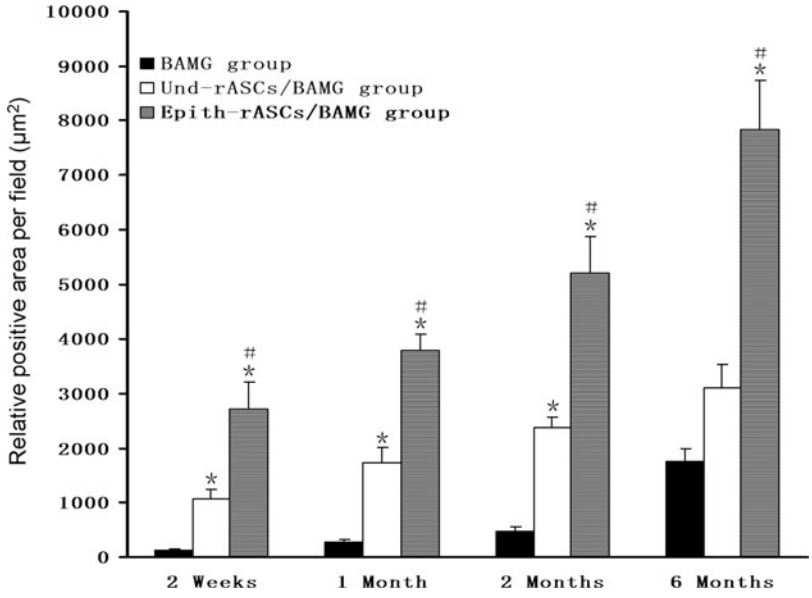

FIG. 8. Epithelial positive areas of *cytokeratin 13* staining at each time point in various groups. $^{*}p < 0.05$ compared with the BAMG group; $^{\#}p < 0.05$ compared with the Und-rASCs/BAMG group. $n = 5$.

postimplantation) was supposed to be a main cause of the contracture of implanted grafts in the BAMG group.

Based on the observations from BrdU labeling, the Epith-rASCs were detected to differentiate into epithelium with the increased expression of *cytokeratin 13* due to the contribution of urethral microenvironment *in vivo*, although terminal differentiation was not achieved after *in vitro* induction. In the Und-rASCs/BAMG group, the contracture of grafts was not efficiently ameliorated, although epithelial differentiation of the implanted cells occurred, which we suggested might be due to that the relatively slow differentiation progress of rASCs in undifferentiated state could not prevent inflammatory cell infiltration and fibrosis of lumen.

Moreover, ASCs have been shown to be available for the treatment of stress urinary incontinence, where injection of the cells is proposed to lead to SMC differentiation *in vivo*.[35,36] In our study, BrdU labeling colocalized with *myosin* expression within the bundles of smooth muscle after rASCs implantation (Fig. 10A–D). Compared with cell-free BAMG implantation (Fig. 10E), increased expression of *myosin* was observed in Epith-rASCs/Und-rASCs seeded BAMG, suggesting that SMC differentiation of rASCs could contribute to the reconstruction of organized muscle bundles in the neourethra.

This study is an initial trial of ASCs as a substitute of urothelium in urethral reconstruction after *in vitro* epithelial induction. Histological and functional evaluation showed that ASCs might be a potential candidate for urethral tissue engineering purposes. But considering in the clinic most patients with urethral stricture combined with local scar contracture and some patients undergo tubularized urethroplasty, these influencing factors may raise the risk of surgery and result in a higher failure rate of repair.

As a major limitation, the complicated design of *in vitro* induction needs to be optimized to reach the mature epithelial differentiation of ASCs. Also, despite the high homology of rASCs and human ASCs, distinction between the original phenotype of two cells may play an important role in cellular differentiation, and as a small animal model, rabbit is less informative for the explanation of the clinical problem, which should gain considerable attention in future investigation. Besides, in long-segment urethral repair (> 2 cm in the rabbits), we believe that the regeneration of the organized muscle layer is necessary for preventing diverticula and fistula, and ASCs may be a suitable option based on the literature[30,37] and the evidence of our study.

Conclusion

The Epith-rASCs have been shown to differentiate into urothelium due to the contribution of urethral microenvironment and be available to prevent lumen contracture and

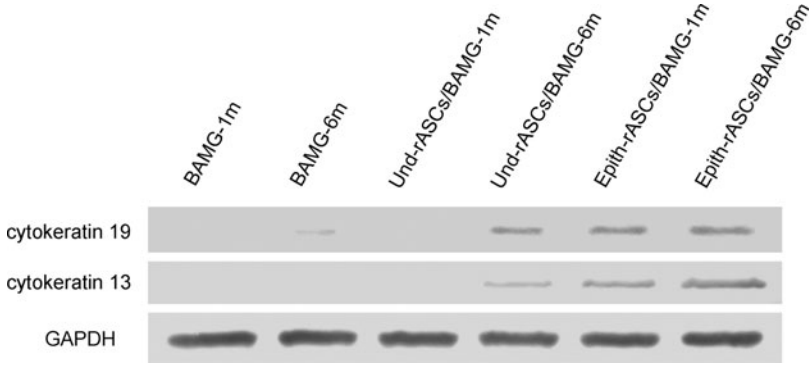

FIG. 9. Expression of epithelial-specific markers (*cytokeratin 19*, *cytokeratin 13*) at 1 and 6 months postimplantation determined by western blot analysis. GAPDH served as the control.

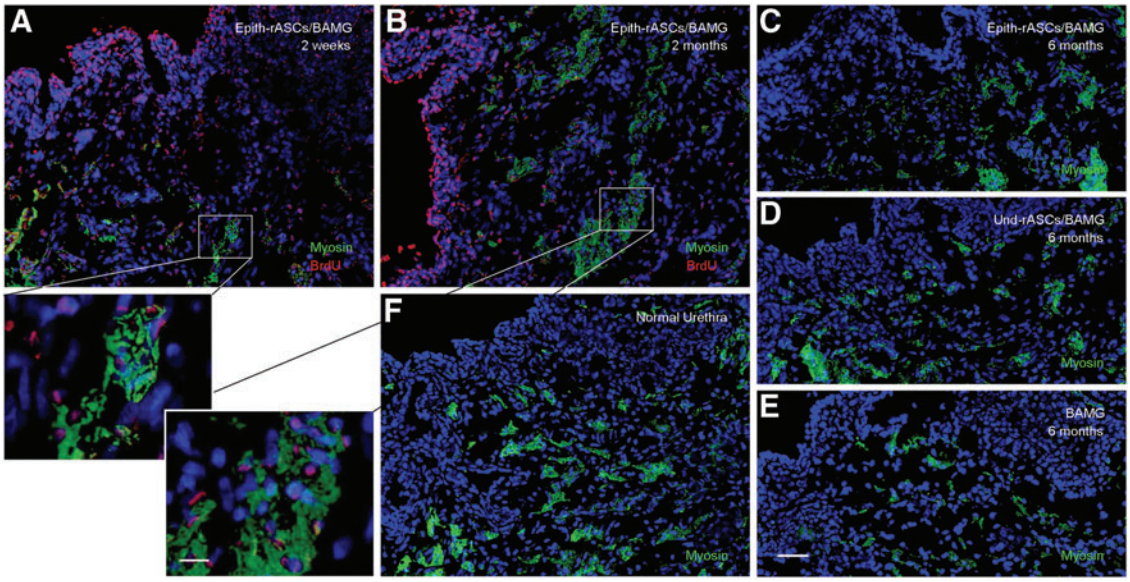

FIG. 10. *Myosin* expression in the neourethra. **(A, B)** BrdU immunostaining in *myosin*-positive cells at 2 weeks **(A)** and 2 months **(B)** postimplantation in the Epith-rASCs/BAMG group. **(C–E)** Immunostaining of *myosin* at 6 months postimplantation in the Epith-rASCs/BAMG group **(C)**, the Und-rASCs/BAMG group **(D)**, and the BAMG group **(E)**, respectively. **(F)** Immunostaining of *myosin* in normal urethra. *Myosin*: green; nuclei of BrdU-labeled cells: red; nuclei of all the cells stained with Hoechst 33258: blue. Scale bars: 50 μm for original figures; 12.5 μm for insets. Color images available online at www.liebertpub.com/tea

subsequent complications, including recurrent stricture postimplantation. These results suggest that ASCs could serve as a potential substitute of urothelium in urethral reconstruction and regeneration studies. Literature showed in male that the urethral epithelium transited into a pseudostratified columnar or stratified columnar epithelium from the neck of the urinary bladder to the distal end.[38,39] For the further investigation of functional effects of implanted cells *in vivo*, the detection of ASCs' barrier gene expression at the ultrastructural level postimplantation would be performed in the next phase of study.

Acknowledgment

This work was financially supported by the Natural Science Foundation of China (grant no.81170641/30901503).

Disclosure Statement

No competing financial interests exist.

References

1. Manzoni, G. Hypospadias repair failures: lessons learned. Eur Urol **49,** 772, 2006.
2. Barbagli, G., Perovic, S., Djinovic, R., Sansalone, S., and Lazzeri, M. Retrospective descriptive analysis of 1,176 patients with failed hypospadias repair. J Urol **183,** 207, 2010.
3. Sievert, K.D., Bakircioglu, M.E., Nunes, L., Tu, R., Dahiya, R., and Tanagho, E.A. Homologous acellular matrix graft for urethral reconstruction in the rabbit: histological and functional evaluation. J Urol **163,** 1958, 2000.
4. De Filippo, R.E., Yoo, J.J., and Atala, A. Urethral replacement using cell seeded tubularized collagen matrices. J Urol **168,** 1789, 2002.
5. Atala, A. Tissue engineering for the replacement of organ function in the genitourinary system. Am J Transplant **4 Suppl 6,** 58, 2004.
6. Selim, M., Bullock, A.J., Blackwood, K.A., Chapple, C.R., and MacNeil, S. Developing biodegradable scaffolds for tissue engineering of the urethra. BJU Int **107,** 296, 2011.
7. Orabi, H., Aboushwareb, T., Zhang, Y., Yoo, J.J., and Atala, A. Cell-seeded tubularized scaffolds for reconstruction of long urethral defects: a preclinical study. Eur Urol **63,** 531, 2013.
8. Fu, Q., Deng, C.L., Liu, W., and Cao, Y.L. Urethral replacement using epidermal cell-seeded tubular acellular bladder collagen matrix. BJU Int **99,** 1162, 2007.
9. Li, C., Xu, Y.M., Song, L.J., Fu, Q., Cui, L., and Yin, S. Urethral reconstruction using oral keratinocyte seeded bladder acellular matrix grafts. J Urol **180,** 1538, 2008.
10. Pittenger, M.F., Mackay, A.M., Beck, S.C., Jaiswal, R.K., Douglas, R., Mosca, J.D., Moorman, M.A., Simonetti, D.W., Craig, S., and Marshak, D.R. Multilineage potential of adult human mesenchymal stem cells. Science **284,** 143, 1999.
11. Barry, F.P., and Murphy, J.M. Mesenchymal stem cells: clinical applications and biological characterization. Int J Biochem Cell Biol **36,** 568, 2004.
12. Weinand, C., Gupta, R., Huang, A.Y., Weinberg, E., Madisch, I., Qudsi, R.A., Neville, C.M., Pomerantseva, I., and Vacanti, J.P. Comparison of hydrogels in the *in vivo* formation of tissue-engineered bone using mesenchymal stem cells and beta-tricalcium phosphate. Tissue Eng **13,** 757, 2007.
13. Hoogduijn, M.J., Crop, M.J., Peeters, A.M., Korevaar, S.S., Eijken, M., Drabbels, J.J., Roelen, D.L., Maat, A.P., Balk, A.H., Weimar, W., and Baan, C.C. Donor-derived mesenchymal stem cells remain present and functional in the transplanted human heart. Am J Transplant **9,** 222, 2009.

14. Brzoska, M., Geiger, H., Gauer, S., and Baer, P. Epithelial differentiation of human adipose tissue-derived adult stem cells. Biochem Biophys Res Commun **330,** 142, 2005.
15. Long, J.L., Zuk, P., Berke, G.S., and Chhetri, D.K. Epithelial differentiation of adipose-derived stem cells for laryngeal tissue engineering. Laryngoscope **120,** 125, 2010.
16. Liu, J., Huang, J., Lin, T., Zhang, C., and Yin, X. Cell-to-cell contact induces human adipose tissue-derived stromal cells to differentiate into urothelium-like cells *in vitro*. Biochem Biophys Res Commun **390,** 931, 2009.
17. Li, H., Xu, Y., Fu, Q., and Li, C. Effects of multiple agents on epithelial differentiation of rabbit adipose-derived stem cells in 3D culture. Tissue Eng Part A **18,** 1760, 2012.
18. Zuk, P.A., Zhu, M., Ashjian, P., De Ugarte, D.A., Huang, J.I., Mizuno, H., Alfonso, Z.C., Fraser, J.K., Benhaim, P., and Hedrick, M.H. Human adipose tissue is a source of multipotent stem cells. Mol Biol Cell **13,** 4279, 2002.
19. Arrigoni, E., Lopa, S., de Girolamo, L., Stanco, D., and Brini, A.T. Isolation, characterization and osteogenic differentiation of adipose-derived stem cells: from small to large animal models. Cell Tissue Res **338,** 401, 2009.
20. Probst, M., Dahiya, R., Carrier, S., and Tanagho, E.A. Reproduction of functional smooth muscle tissue and partial bladder replacement. Br J Urol **79,** 505, 1997.
21. Dahms, S.E., Piechota, H.J., Dahiya, R., Lue, T.F., and Tanagho, E.A. Composition and biomechanical properties of the bladder acellular matrix graft: comparative analysis in rat, pig and human. Br J Urol **82,** 411, 1998.
22. Li, C., Xu, Y., Song, L., Fu, Q., Cui, L., and Yin, S. Preliminary experimental study of tissue-engineered urethral reconstruction using oral keratinocytes seeded on BAMG. Urol Int **81,** 290, 2008.
23. Ji, S.Z., Xiao, S.C., Luo, P.F., Huang, G.F., Wang, G.Y., Zhu, S.H., Wu, M.J., and Xia, Z.F. An epidermal stem cells niche microenvironment created by engineered human amniotic membrane. Biomaterials **32,** 7801, 2011.
24. Palminteri, E., Berdondini, E., Colombo, F., and Austoni, E. Small intestinal submucosa (SIS) graft urethroplasty: short-term results. Eur Urol **51,** 1695, 2007.
25. Springer, A., and Subramaniam, R. Preliminary experience with the use of acellular collagen matrix in redo surgery for urethrocutaneous fistula. Urology **80,** 1156, 2012.
26. Hauser, S., Bastian, P.J., Fechner, G., and Müller, S.C. Small intestine submucosa in urethral stricture repair in a consecutive series. Urology **68,** 263, 2006.
27. Bhargava, S., Patterson, J.M., Inman, R.D., MacNeil, S., and Chapple, C.R. Tissue-engineered buccal mucosa urethroplasty-clinical outcomes. Eur Urol **53,** 1263, 2008.
28. Rheinwald, J.G., and Green, H. Serial cultivation of strains of human epidermal keratinocytes: the formation of keratinizing colonies from single cells. Cell **6,** 331, 1975.
29. Baer, P.C. Adipose-derived stem cells and their potential to differentiate into the epithelial lineage. Stem Cells Dev **20,** 1805, 2011.
30. Wang, C., Yin, S., Cen, L., Liu, Q., Liu, W., Cao, Y., and Cui, L. Differentiation of adipose-derived stem cells into contractile smooth muscle cells induced by transforming growth factor-beta1 and bone morphogenetic protein-4. Tissue Eng Part A **16,** 1201, 2010.
31. Choi, Y.S., Vincent, L.G., Lee, A.R., Dobke, M.K., and Engler, A.J. Mechanical derivation of functional myotubes from adipose-derived stem cells. Biomaterials **33,** 2482, 2012.
32. Kroeze, R.J., Knippenberg, M., and Helder, M.N. Osteogenic differentiation strategies for adipose-derived mesenchymal stem cells. Methods Mol Biol **702,** 233, 2011.
33. Mahmoudifar, N., and Doran, P.M. Chondrogenic differentiation of human adipose-derived stem cells in polyglycolic acid mesh scaffolds under dynamic culture conditions. Biomaterials **31,** 3858, 2010.
34. Estes, B.T., Diekman, B.O., Gimble, J.M., and Guilak, F. Isolation of adipose-derived stem cells and their induction to a chondrogenic phenotype. Nat Protoc **5,** 1294, 2010.
35. Zhao, W., Zhang, C., Jin, C., Zhang, Z., Kong, D., Xu, W., and Xiu, Y. Periurethral injection of autologous adipose-derived stem cells with controlled-release nerve growth factor for the treatment of stress urinary incontinence in a rat model. Eur Urol **59,** 155, 2011.
36. Wu, G., Song, Y., Zheng, X., and Jiang, Z. Adipose-derived stromal cell transplantation for treatment of stress urinary incontinence. Tissue Cell **43,** 246, 2011.
37. Zhao, Z., Yu, H., Xiao, F., Wang, X., Yang, S., and Li, S. Differentiation of adipose-derived stem cells promotes regeneration of smooth muscle for ureteral tissue engineering. J Surg Res **178,** 55, 2012.
38. Romih, R., Jezernik, K., and Masera, A. Uroplakins and *cytokeratins* in the regenerating rat urothelium after sodium saccharin treatment. Histochem Cell Biol **109,** 263, 1998.
39. Romih, R., Korosec, P., de Mello, W., Jr., and Jezernik, K. Differentiation of epithelial cells in the urinary tract. Cell Tissue Res **320,** 259, 2005.

Address correspondence to:
Yuemin Xu, PhD, MD
Department of Urology
Sixth People's Hospital
Jiao Tong University of Shanghai
600 Yi Shan Road
Shanghai 200233
P.R. China

E-mail: urology600@gmail.com

Received: February 17, 2013
Accepted: September 25, 2012
Online Publication Date: January 16, 2014